НАУЧНО-ТЕХНИЧЕСКИЙ ВЕСТНИК ИНФОРМАЦИОННЫХ ТЕХНОЛОГИЙ, МЕХАНИКИ И ОПТИКИ
ноябрь–декабрь 2023 Том 23 № 6 http://ntv.ifmo.ru/
SCIENTIFIC AND TECHNICAL JOURNAL OF INFORMATION TECHNOLOGIES, MECHANICS AND OPTICS
November–December 2023 Vol. 23 No 6 http://ntv.ifmo.ru/en/
ISSN 2226-1494 (print) ISSN 2500-0373 (online)

doi: 10.17586/2226-1494-2023-23-6-1223-1232

Convective heat transfer and hydrodynamics of flow at the endwall around a turbine blade under the influence of a magnetic field

Kozhikkatil Sunil Arjun[1]✉, Porathoor Sunny Tide[2]

[1,2] Division of Mechanical Engineering, School of Engineering, Cochin University of Science and Technology, Kochi, 682022, India

[1] arjunks@cusat.ac.in✉, https://orcid.org/0000-0003-1832-3759
[2] tideps@cusat.ac.in, https://orcid.org/0000-0002-8061-113X

Abstract

The present study analyses the influence of magnetohydrodynamics on endwall heat transfer in turbine blades using computational fluid dynamics simulations. The simulations consider the three-dimensional geometry of the turbine blade, the magnetic intensity, and the boundary conditions. The outcome revealed the existence of a magnetic field can outstandingly increase the pitch-averaged film cooling effectiveness and endwall heat transfer, particularly near the edges of the turbine vane with an optimal magnetic field. This results in a more uniform distribution of heat transfer along the endwall and can help to reduce hot spots and prevent thermal damage to the blade. The research also highlights the importance of considering the magnetic intensity and its impact on the flow characteristics and heat transfer when designing turbine blades for high-speed applications. By optimizing the design of the turbine blades to take into account the magnetohydrodynamic effect, engineers can improve the overall performance and lifespan of these critical components. Numerical simulations had been utilized to forecast the impacts of contouring of endwalls efficiently, employing the secondary kinetic energy coefficient as the accomplished parameter demonstrated in the current investigation. A reduction in endwall heat load with enhanced net heat flux reduction and aerodynamic performance is reported for a non-axisymmetrically contoured endwall subjected to optimal magnetic field strength. The novelty of the present study is the establishment of the impact of vortices on endwall heat transfer with respect to the vane under the influence of magnetohydrodynamics to reduce the weight and cost of a turbine engine.

Keywords

non-axisymmetric contouring, magnetohydrodynamics, net heat flux reduction, aerodynamic performance, secondary kinetic energy

For citation: Arjun K.S., Tide P.S. Convective heat transfer and hydrodynamics of flow at the endwall around a turbine blade under the influence of a magnetic field. *Scientific and Technical Journal of Information Technologies, Mechanics and Optics*, 2023, vol. 23, no. 6, pp. 1223–1232. doi: 10.17586/2226-1494-2023-23-6-1223-1232

УДК 532.51

Конвективный теплообмен и гидродинамика течения у торцевой стенки лопатки турбины под действием магнитного поля

Кожиккатил Сунил Арджун[1]✉, Поратур Санни Тайд[2]

[1,2] Отделение машиностроения, инженерная школа, Кочинский университет науки и технологий, Кочи, 682022, Индия

[1] arjunks@cusat.ac.in✉, https://orcid.org/0000-0003-1832-3759
[2] tideps@cusat.ac.in, https://orcid.org/0000-0002-8061-113X

Аннотация

Выполнен анализ влияния магнитогидродинамики на теплообмен на торцевых стенках лопаток турбины с использованием компьютерного моделирования. При моделировании учтена трехмерная геометрия лопатки турбины, напряженность магнитного поля и граничные условия. Результат моделирования показал, что существование магнитного поля может значительно повысить эффективность пленочного охлаждения в среднем на шаг и теплообмен на торцевой стенке, особенно вблизи краев лопатки турбины с оптимальным магнитным полем. Это приводит к более равномерному распределению теплопередачи вдоль торцевой стенки

и может помочь уменьшить количество горячих точек и предотвратить термическое повреждение края лопатки турбины. Исследование показало необходимость учета напряженности магнитного поля и его влияние на характеристики потока и теплопередачу при проектировании лопаток турбин для высокоскоростных применений. Оптимизируя конструкцию лопаток турбины с учетом магнитогидродинамического эффекта, инженеры могут улучшить общую производительность и срок службы этих критически важных компонентов. Численное моделирование применено для эффективного прогнозирования последствий контурирования торцевых стенок с использованием коэффициента вторичной кинетической энергии в качестве окончательного параметра, полученного в результате выполненного анализа. Показано снижение тепловой нагрузки на торцевую стенку лопасти турбины с уменьшением чистого теплового потока и улучшение аэродинамических характеристик торцевой стенки с неосесимметричным контуром, подвергнутой воздействию магнитного поля оптимальной напряженности. В работе продемонстрировано влияние вихрей на теплообмен торца относительно лопатки под воздействием магнитогидродинамики для снижения массы и стоимости газотурбинного двигателя.

Ключевые слова

неосесимметричное контурирование, магнитогидродинамика, уменьшение чистого теплового потока, аэродинамические характеристики, вторичная кинетическая энергия

Ссылка для цитирования: Арджун К.С., Тайд П.С. Конвективный теплообмен и гидродинамика течения у торцевой стенки лопатки турбины под действием магнитного поля // Научно-технический вестник информационных технологий, механики и оптики. 2023. Т. 23, № 6. С. 1223–1232 (на англ. яз.). doi: 10.17586/2226-1494-2023-23-6-1223-1232

Introduction

Heat transfer in magnetohydrodynamic (MHD) endwall contouring in turbine blades is a significant and novel research area with several potential applications in the field of power generation. Endwall contouring of the turbine is a method used in gas turbines to control the flow of air and improve turbine efficiency [1]. By applying a magnetic field to the fluid, the fluid is forced to move in a particular direction, which can be used to control the flow [2]. The effects of the magnetic field applied transversely to the direction of the steady turbulent flow could observe the flow field control and heat transfer when numerically studied [3]. The magnetic intensity required for the flow control can be quite low, and the magnetic field can interfere with the operation of other heat transfer components in the flow [4]. Additionally, the design and implementation of an MHD system can be complex and expensive [5]. Nonaxisymmetric endwalls are getting universal status owing to their accomplished competencies, changing the characteristics of the secondary flow and altering the film cooling potential with respect to endwalls.

The convective heat transfer and hydrodynamics of flow under the effect of low magnetic field strength can affect the boundary layer development, flow separation, and turbulence intensity, which in turn can modify the average Nusselt number (*Nu*) increase of more than 10 % by Hartmann number (*Ha*) of 12 [6]. The Lorentz forces induced by the magnetic field can also modify the flow patterns and velocity profiles, leading to changes in the rotating disk pressure distribution and drag coefficient [7]. The extent of these modifications depends on the impacts of the strength and orientation of the magnetic field, the fluid properties, and the geometry on the thermal exchange of nanofluid flow over a plate [8]. The impact of slip as well as MHD of a layer of flow boundary on the thermal exchange across a plate in motion is investigated using the generation of distinct entropy by numerical simulations [9]. The effects of MHD on the nanofluid flow and heat transfer in a stretchable surface are analyzed using Computational Fluid Dynamics (CFD) simulations [10] and found to significantly reduce the separation bubble size and enhance its impact on heat transfer.

The use of MHD for thermal exchange augmentation over a two-way, proliferating, stretching sheet of a permeable nature, using a channel flow with a magnetic field applied parallel to the flow direction was investigated [11]. Aerothermal revamping of film cooling hole regions at the squealer tip of a high-pressure turbine vane using CFD simulations is optimized for cooling effectiveness and aerodynamic performance [12]. The influence of MHD on the heat transfer of a curved blade with turbulators in a 3D duct using numerical simulations is examined [13]. The external magnetic field exerting towards the gradient of temperature has an outstanding effect on thermal exchange and hence should be taken into account when designing for high-speed applications with a channel flow [14]. A rectangular duct with a magnetic field applied perpendicular to the flow direction was investigated [15] and found that the MHD system improved the fluid mixing and reduced the separation bubble size, leading to a maximum heat transfer enhancement. The *Nu* diminishes as the *Ha* rises beyond a critical value [16] in a swirling flow due to a rotating disk of a cylindrical enclosure. A detailed turbine flow modeling at low and high turbulence intensities is performed concerning the heat transfer and hydrodynamics in 3D throughout the optimization by numerical simulations and the impacts of the different secondary flow structures on the endwall thermal exchange are described in depth [17].

The secondary kinetic energy coefficient (C_{ske}) was distinctly observed to be the best factor for the study objective. An acuminate elevation in C_{ske} (150 % at incidence 5°) at the vane row downstream with 50 % of the axial chord plane was distinguished [18]. Delineated the rotor allied angle of exit flow angle, coefficient of loss, as well as the C_{ske} as the best productive criteria for designating the impacts of the shape deviations of the endwall contouring as well as efficiency, while other parameters indicated the load variation [19]. The helicity parameter cannot be optimized in comparison with C_{ske}, a drawback established [20] and suggests

that concerning the turbine, the helicity parameter is not suitable [19]. Nonaxisymmetric contouring of the endwall can outstandingly increase the productive extent of the purge flow area by up to 28.29 %, and the endwall adjacent to the suction surface can attain greater cooling potential [21]. The establishment tendencies of succeeding-generation turbine vane cooling mechanisms, in excess of 2000 K temperature, include the progressive revealing of enhanced efficiency complex cooling arrangement as well as manifold objective collective cooling composition [22].

Some of the key research gaps include a lack of experimental validation, limited understanding of the interaction between MHD and other turbine components (blade and cooling system), optimization of MHD parameters, assessment of long-term durability and maintenance requirements, and investigation of potential safety concerns. Further research is needed to optimize the magnetic intensity, the direction of the magnetic field as well as endwall composition to determine the most effective configurations for MHD in turbine endwall contouring. Further incrementing models concerning 3D printing, complex cooling composition models, and incrementing in response with the artificial intelligence algorithm is also of importance. Monitoring the cooling performance of fresh cooling media as well as heat pipes, consolidated heat conservation with fresh heat insulators, and the execution of diminished resistance and elevated productive dimpled surface cooling are also pivotal. The non-axisymmetrically contoured endwall heat load reduction with better net heat flux reduction and aerodynamic performance at an optimal magnetic field strength is the innovativeness of this investigation.

The span of MFR so far reported is inadequate for the beneficial accomplishment of cooling the passage concerning the Nozzle Guide Vane (NGV). The endwall pressure surface substantiates that the coolant amenability to accomplish the zone is extremely crucial. Furthermore, the cavity of fishmouth in the passage of NGV-combustor creates a cavity vortical structure of 3D nature that carries away the coolant towards the pitch route. A higher step height due to combustor-NGV misalignment necessitates elevated momentum of coolant to control the vortices generated through various steps. The vortices prevent the upstream coolant from reaching the NGV passage. In addition, the movement sequence of the coolant is contingent on its blow rate. Diminishing the density ratio or enhancing the Blowing Ratio (BR) leads to elevated momentum of coolant, and can help the jets of coolant smother the Horseshoe Vortex (HV) additionally, but also cause more lift-off, mitigating the coolant reattachment which adversely affects the cooling performance. This study is aimed to brighten the knowledge on gas turbine cooling at regions on the endwall that have the greatest outstanding influence on the aerodynamic or endwall thermal exchange accomplishments. In the current investigation, collaboration is established connecting mainstream as well as purge flow upon non-axisymmetric contouring of endwall. The novelty of the present study is the establishment of the impact of a 3D vortical structure on turbine endwall heat transfer to reduce the weight and cost of a turbine engine. The present study reduces the endwall heat load of the vane and improves the overall efficiency of the turbine. The present study forms the first report on the impact of MHD on endwall heat transfer in respect of turbine vane.

Research methodology

The simulations are typically conducted using a three-dimensional model (Fig. 1) of the turbine blade with MHD effects taken into account using CFD software on endwall heat transfer in turbine blades. The simulations consider the geometry of the turbine blade, the boundary conditions, and magnetic intensity, and the results are typically analyzed using the Nu. The magnetic field is applied around the blade in the direction of the rotation of the blade. Though predictions using Shear Stress Transport (SST) Transition models were a high replica of experimental values concerning secondary flow regions and heat transfer, the suction side trailing edge turbulence transition could not be evidenced. High-fidelity secondary flow simulations of the vane cascade passage are rare due to the high cost and lack of experimental data. A shape function and cooling hole positions were optimized from an efficient turbine endwall cooling by multi-fidelity simulations. The size and strength of the vortex and hence the endwall heat transfer were over-predicted by the Reynolds-averaged Navier–Stokes (RANS) models and hence periodic corrections and improvements are inevitable. The $Re_{\theta\text{-}\gamma}$ model can utilize only the local information and correlations of experimental data that cause the transition.

The $Re_{\theta\text{-}\gamma}$ transition model accurately predicts boundary layers of bound and leniently parted in the zone of transition, while its correctness lowers for densely parted flows. To enhance the forecast of the accomplishment at the design scale, at which laminar as well as turbulent flow zones frequently exist concurrently on the vanes, two models viz., the SST eddy-viscosity turbulence model which takes care completely the transition of flow, and the $Re_{\theta\text{-}\gamma}$ transition model which solves for predicting flow transition are used together. The fresh turbulence closure integrates the advantages of both models exercising an approach of additive hybrid filtering. This combination model has several relatively minor variations in the eddy-viscosity definition that employs the rate of strain alternately with the vorticity magnitude. This procedure has the prospective for correctly securing densely parted layers of boundary in the transitional span of Re at a judicious calculation expense. The transitional hybrid approach secures the physics analogous with a parted wake over a span of Re 10 to $2 \cdot 10^6$ and is superiorly recommended in securing accomplishment and flowfield characteristics of engineering attraction than persisting turbulence models. It leads to a reduction of the numerical uncertainty (discretization errors) and the sharpest transition.

A linear vane cascade is simulated by Ansys Fluent[1] with the RANS model combining SST eddy viscosity [23] with the $Re_{\theta\text{-}\gamma}$ model [24] for the flow field around the

[1] Fluent FLUENT User's Guide, New Hampshire, USA, FLUENT Inc., 2003. Available at: https://www.archive.org/details/ANSYSFluentUsersGuide (accessed: 15.11.2023).

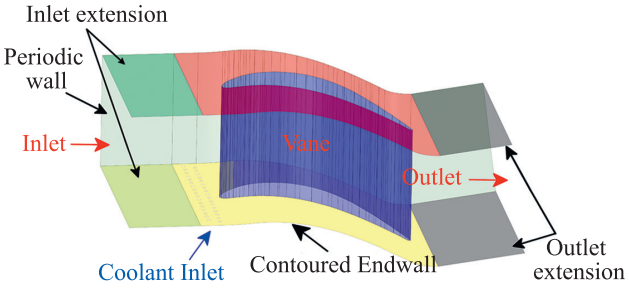

Fig. 1. Schematic diagram of the linear vane cascade

blade with non-axisymmetric contouring of the endwall, thermal exchange, and magnetic field. Two different endwall shapes viz. flat and contoured (axisymmetric convergent) designed for the first NGV were investigated in this study. The computational domain has 16 % inlet turbulence, $1.7 \cdot 10^6$ outlet *Re*, and 0.85 outlet Mach number. The upstream purge flow is considered by the 42 cylindrical cooling double-row holes with a diameter of 2.4 mm which are located at 0.4 C_{ax} upstream of the center passage vane leading edge.

The mesh size of the CFD model (Fig. 2) used in endwall contouring and magnetic field studies of turbine blades depends on several factors, such as the vane geometry, the flow conditions, the turbulence model used, and the accuracy required in the simulation. A nested grid is used for the vane surface proximity grid refining and on the pressure surface as well as the boundary layer of streamwise trajectory. Meshes of a structured nature were created through Integrated Computer-aided Engineering and Manufacturing (ICEM) CFD with low *Re* meshes with nodes of $6 \cdot 10^6$ for the axisymmetric convergent contoured endwall vane passage, and $9 \cdot 10^6$ for the coolant holes as well as the plenum. For the locations of the boundary layer of the wall, meshes were concentrated using a height of $1.5 \cdot 10^{-3}$ mm for the first cell and a 1.15 expansion factor to reproduce the flow evolution. The *y*+ value was maintained lower than 0.8 on the endwall. Film cooling effectiveness (FCE) spread around the vane leading edge on the contoured endwall with $6 \cdot 10^6$, $9 \cdot 10^6$, $12 \cdot 10^6$, and $15 \cdot 10^6$ grid points were compared at 2.5 % BR. The FCE value of 0.48 was unchanged when the grid number increased from

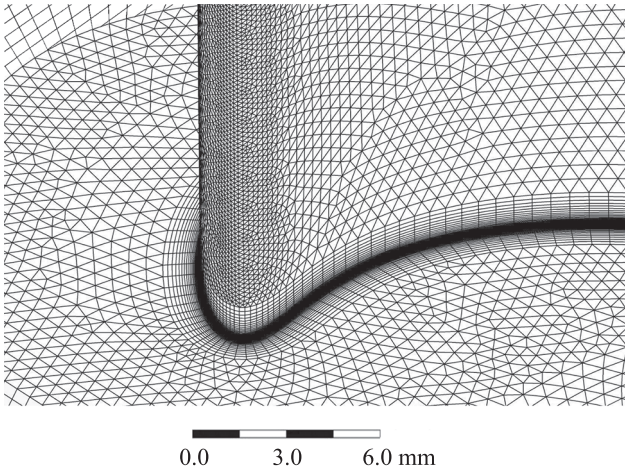

Fig. 2. Mesh details of the contoured vane endwall

$12 \cdot 10^6$ to $15 \cdot 10^6$. The mesh size was fine enough to resolve the layer of boundary adjacent to the blade surface and the turbulence structures in the flow field and consistent throughout the domain. Grid-independent endwall film cooling effectiveness was evident with a $12 \cdot 10^6$ mesh size. The Root Mean Square (RMS) error in the predictions is 9 %. Convergence is checked with the RMS below 10^{-6} upon termination after 2400 iterations.

Conditions of adiabatic and no-slip wall boundary had been assigned with respect to the holes as well as the plenum of coolant. The coolant temperatures were set as 298 and 295 K. The near endwall film flow temperatures are equal to the adiabatic wall temperatures. A uniform wall temperature of 300 K was applied. Periodic boundary conditions were assigned over the computational domain boundary towards the pitch-ward direction to simulate periodic flow or temperature fields in the computational domain. A thin Blasius boundary layer is imposed at the inlet with $Re_x = 2 \cdot 10^5$. Consistent Neumann boundary conditions to the velocity, temperature, and pressure fields, and No-slip boundary conditions to the vane and endwalls are imposed. Uniform heat flux to the vane, endwall heating condition of the leading edge, and an adiabatic condition at its upstream are provided. Pressure–velocity coupling using a pressure-based method was used.

Film cooling introduces a cooler secondary fluid onto the external surface of a component to shield it from high-temperature gases by creating a thin protective layer that reduces heat transfer and prevents direct contact with hot gases. The coolant mixes with the boundary layer without significantly increasing turbulence or entraining additional hot freestream gas. The *Nu* and the effectiveness of adiabatic film cooling (η) with respect to the endwall are found utilizing the following equations:

$$Nu = \frac{h_c C}{k},$$

$$\eta = \frac{T_{aw,c1} - T_{aw,c2}}{T_{c1} - T_{c2}}.$$

Here, h_c is the Heat Transfer Coefficient (HTC), C is the NGV chord length and k is the thermal conductivity. The adiabatic wall temperatures, $T_{aw,c1}$, and $T_{aw,c2}$ are at the first (T_{c1}) and second (T_{c2}) coolant temperatures.

The heat transfer coefficient is defined as the coefficient of proportion, connecting the heat flux as well as the thermodynamic operating force for the heat flow.

$$h = q/\Delta T,$$

where q represents the heat flux or thermal power in an area of unity and ΔT is the temperature deviation connecting the surface of the solid and the adjacent area of fluid.

Reynolds number (*Re*) is defined as the fraction of forces of inertia to viscosity inside the fluid, which is amenable to comparative inner motion owing to various velocities of fluid.

$$Re = \rho u L/\mu,$$

where ρ represents the fluid density, u denotes the speed of the flow, L represents the specific length, and μ denotes the fluid dynamic viscosity.

The Hartmann number (Ha) is the ratio of electromagnetic force to the viscous force.

$$Ha = BL\sqrt{\frac{\sigma}{\mu}},$$

where B denotes the intensity of the magnetic field, L represents the specific length, σ denotes the electrical conductivity, and μ represents the fluid dynamic viscosity.

The Net Heat Flux Reduction (NHFR) denotes an absolute appraisal of the endwall thermal load and is estimated using the FCE and HTC (h) as follows:

$$NHFR = 1 - h/h_0(1 - \eta\varphi),$$
$$\varphi = T_\infty - T_c/T_\infty - T_w,$$

where h_0 denotes heat transfer coefficient without film cooling, φ represents the effectiveness of cooling on an overall basis denoted by non-dimensional metal temperature, T_∞ is the freestream temperature, T_c is the coolant temperature and T_w is the wall temperature. For a turbine vane with film cooling, its value is set as 1.6 [25].

The Total Pressure Loss Coefficient (TPLC) is a measure of aerodynamic performance and is calculated as the fraction of the total pressure drop by the variation in static and incoming pressure. TPLC with coolant blowing are:

$$TPLC = \frac{\frac{\dot{m}_c}{\dot{m}_c + \dot{m}_m}P_{t,cin} + \frac{\dot{m}_c}{\dot{m} + \dot{m}_m}P_{t,m} - P_{t,f}}{P_{t,m} - P_f}.$$

Coolant mass flow rate is denoted $\dot{m}_c$, mainstream mass flow rate $\dot{m}_m$, coolant inlet total pressure $P_{t,cin}$, mainstream total pressure $P_{t,m}$, mixed flow total pressure $P_{t,f}$ and mixed flow static pressure P_f. No slot leakage is seen with a zero value of $\dot{m}_c$.

The C_{ske} is formulated [26] as:

$$C_{ske} = \frac{V_{sec}^2 + V_r^2}{V_{in}^2},$$

where:

$$V_{sec} = V\sin(\alpha - \alpha_{mid}),$$

V represents absolute velocity concerning secondary, relative reference, and inlet. α_{mid} is substituted with the angle of flow at the exit denoted as α by its scalar mean.

A comparison with the experiment measurements [27] provided a good agreement at a Mass Flux Ratio (MFR) of 2.5 along the middle pitch for axisymmetric convergent contoured endwall Nu distributions (Fig. 3). An enhanced thermal exchange is not well forecasted owing to the impact of the HV leg concerning the suction surface. A deterministic unsteadiness might also contribute to the measured turbulent kinetic energy since the HV has a bimodal nature. This concentrated turbulent kinetic energy might have resulted in the gradients of heat transfer. The numerical predictions in general show a good agreement with measurements in trend, the magnitude has differences concerning upstream locations of the vane leading edge

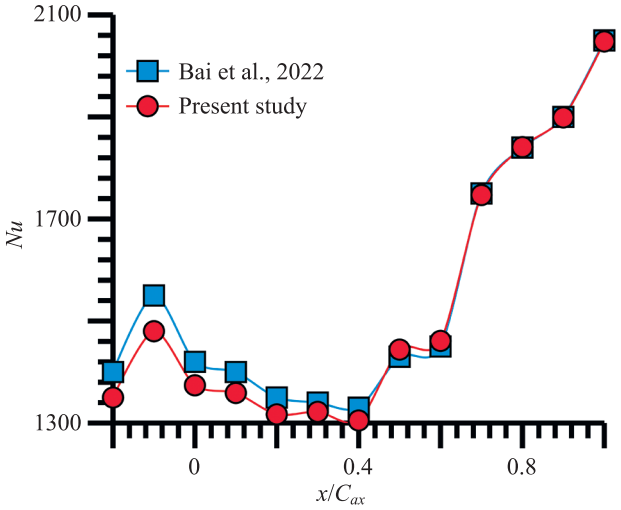

Fig. 3. Validation of Nu at MFR 2.5 along the middle pitch for contoured endwall

($x < 0$). The maximum prediction error is less than 19 % in the whole vane passage ($0 < x/C_{ax} < 0.65\ C_{ax}$) and less than 1.24 % downstream of the vane passage throat ($x > 0.65\ C_{ax}$). This prediction error might be caused by the surface roughness in the original measurements, (but treated as a smooth one in simulations) as well as the insufficient prediction of endwall secondary flows. In general, the present numerical method is reliable. It can be used to investigate the impacts of axisymmetric convergent contouring and BR on film cooling as well as the associated phantom cooling distributions on the endwall, turbine stage efficiency, heat transfer, and aerodynamic performances of the vane pressure side. Several authors reported the existence of maximum prediction error in a contoured endwall to the tune of 20 % and an extreme deviation, especially in locations having elevated skew (greater than 70 degrees) as well as adverse gradients of pressure downstream of HV separation and reattaching flow due to adequately capturing the physics of complex flow [27].

Results and discussion

The secondary flow patterns can be further modified due to the interaction between the magnetic field and the electrically conductive fluid in the blade. By increasing the heat transfer, the MHD effect can help to reduce the temperature of the blade, leading to the thermal stress lowering and extending the lifespan of the blade. The increased heat transfer can be used to improve the cooling effectiveness of the blade, which can help to prevent thermal damage and improve the overall performance.

Impact of magnetohydrodynamics on Pitch-averaged endwall film cooling effectiveness

To quantify the film cooling benefit for the entire endwall surface, pitch-averaged endwall film cooling effectiveness, $\overline{\eta}$ for non-axisymmetrically contoured endwall at MFR 1.5 % is depicted in Fig. 4. The endwall η rapidly increases (1.2 to 2.3 %) as Ha increases from 25 to 75, because the HV is suppressed by the high momentum coolant. As the Ha increases from 75 to 100, a reduction in endwall $\overline{\eta}$ is observed (almost equal to or lower than that

for *Ha* 25). The non-axisymmetric convergent contouring is beneficial for the endwall $\overline{\eta}$, but the level of benefit is significantly affected by the *Ha*. The level of benefit first increases then decreases with the increasing *Ha*, and the maximum increase (2.3 %) is noticed around the vane leading edge at *Ha* 75. Elevation of the endwall-specific thermal load because of the coolant jet merging is evident in contoured geometry with the MFR 0.5 and 1.0 %. But the zone is migrated further downstream than in the flat endwall. An elevated flow rate of coolant markedly lowers the thermal load adjacent to the upstream location and the leading edge for the contoured endwall with an MFR of 1.5 %. At elevated MFR, superior cooling is achieved adjacent to the region of stagnation of the leading edge. The coolant spread in the direction of the mainstream is not elevated much for MFR 1.5 % in comparison with 1.0 % because of the coolant lift-off from the endwall. The *Nu* contours for MFR 1.5 % with extremely elevated zones of heat transfer corroborate this behavior and might be because of higher turbulence amalgamation of coolant and mainstream. In the case of the contoured endwall, the spread of coolant film is much more elevated over the airfoil suction side in the streamwise direction than the flat endwall for elevated coolant MFR. This phenomenon might be because of the adherence of the coolant with the endwall by the impact of contouring at the passage downstream with not much influence of the secondary flow. At 1.5 % MFR, the flat endwall has slightly elevated effectiveness at the leading-edge forepart. But the contoured endwall has markedly elevated effectiveness at the leading-edge forepart at 0.5 and 1.0 % MFR.

Impact of magnetohydrodynamics on thermal exchange

As the *Ha* magnetic fields are elevated in the range of 25–75, a significant diminishing impact on endwall *Nu* in turbine blades is noticed to the tune of 1.3 % to 2.3 % (Fig. 5). The magnetic field acts to suppress the turbulence in the flow near the endwall leading to a more laminar flow regime and diminished *Nu*. However, high Hartmann number magnetic fields can also lead to increased pressure drop and flow resistance, which can reduce the gross productivity of the turbine blade. When *Ha* is enhanced to 100, the reduction in *Nu* is lowered to 1.2 % (lower than that at *Ha* 25). Therefore, *Ha* 75 has an optimal magnetic field strength that diminishes the *Nu* while minimizing the associated losses. Increasing the Hartmann number from 0 to 75 resulted in an approximately 2.3-fold decrease in the *Nu* on the endwall of a turbine blade. As the Hartmann number increases, the magnetic field becomes stronger and can suppress turbulence in the flow leading to a more laminar flow regime. Increasing the Hartmann number to 25 can result in the formation of multiple vortex structures including Dean vortices and counter-rotating streamwise vortices. These vortex structures can enhance heat transfer near the endwall by promoting the mixing of the fluid and increasing the convective HTC. The augmentation in thermal exchange near the vane edges results in a more uniform distribution of heat transfer along the endwall, which can help to reduce hot spots and prevent thermal damage to the blade being beneficial for improving the overall performance of turbine blades.

Impact of magnetohydrodynamics on net heat flux reduction

A non-axisymmetrically contoured endwall significantly augments the NHFR when the MFR is greater than 1.0 % leading to a diminished heat load on the endwall than a flat one. An elevated NHFR explains a lower heat load on the endwall. The NHFR has the main gain from the lowering of heat transfer than the augmentation in film cooling at MFR 0.5 % and hence the NHFR enhancement is not very beneficial. At MFR 1.0 %, an endwall with a non-axisymmetrically contoured geometry considerably enhances the NHFR at an axial coordinate/axial chord length, $x/C_{ax} < 0.65$ with a still elevated value upstream. A 1.5 % contouring amplitude achieves the highest NHFR throughout the endwall and might be due to augmenting the FCE and lowering the rates of heat transfer. At $x/C_{ax} < 0.65$ with MFR 1.5 %, the NHFR gets augmented continuously for a non-axisymmetrically contoured endwall. The peak NHFR is accomplished at almost all endwall locations with a 1.0 % amplitude of contouring. The NHFR at the endwall front gets lowered with the escalation of the amplitude of contouring.

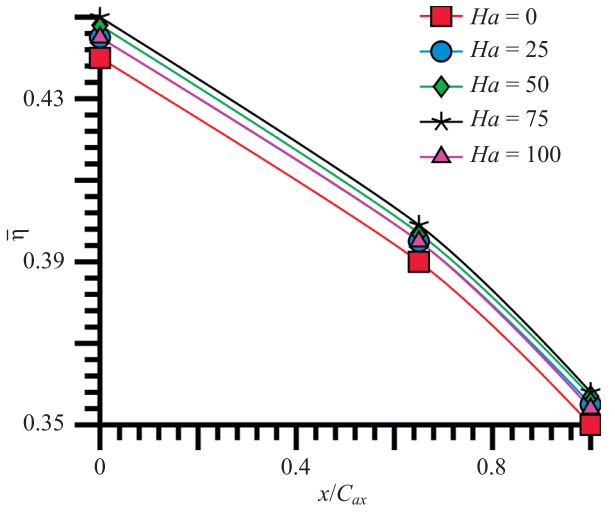

Fig. 4. Impact of magnetic flux on Pitch-averaged endwall film cooling effectiveness at MFR = 1.5 %

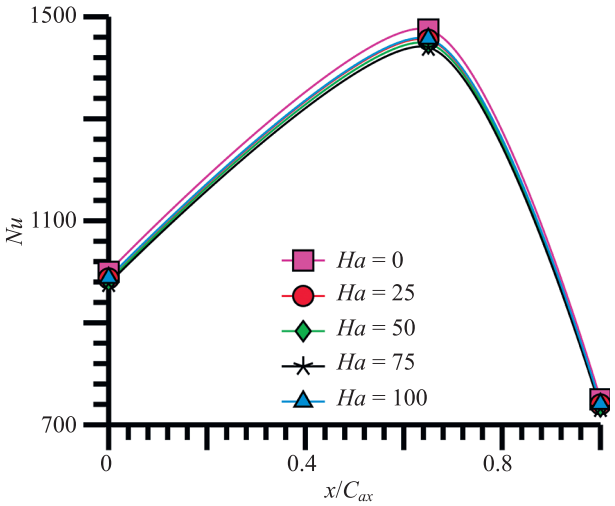

Fig. 5. Impact of magnetic flux on *Nu* at MFR = 1.5 %

Adiabatic cooling effectiveness is more on endwall with contoured geometry than that with flat geometry at similar MFR. Since the contoured endwall has a wide area for cooling, the enhanced cooling performance benefit in the passage vanishes. However, the impact of effectiveness enhancement in adiabatic cooling is higher, compared to the area change, leading to a lower endwall net heat flux in comparison to that in the passage, when MFR > 1.625 %. The marked augmentation in NHFR (Table) at the endwall of non-axisymmetrically contoured geometry with the introduction of magnetic flux from *Ha* 25 to 75 at MFR 1.5 % is the outcome of diminishing the strength of the vortex in the passage by beneficially dominating the secondary flow as well as by lowering the cross-passage flow gradients and the competency of the coolant film in penetrating far up to the trailing edge. The drop in local HTC at augmented pressure side NHFR recorded a range of 1.6% to 2.63 % at *Ha* 25 to 75 and a further drop to 1.05 % at *Ha* 100. The current study thus established the optimal magnetic intensity as *Ha* 75. The effect of the dissemination of coolant film is thus dominating towards the platform suction surface as well as towards the slot stagnation region downstream. An enhanced overall *Nu* is found at MFR 0.5–1.0 % with the non-axisymmetrically contoured endwall, marked augmentation in NHFR can be acquired since the FCE is elevated than the flat endwall. At 1.5 % MFR, the performance of a contoured geometry is higher as coolant film adheres with the surface by contouring, and for flat geometry, jet lift-off takes place. A contoured geometry considerably augments the endwall NHFR airfoil (averaged crosswise at the direction of length) at MFR >1.0 %. Hence, a contoured geometry can lower the endwall heat load than a flat geometry.

Impact of magnetohydrodynamics on aerodynamic performance

Fig. 6 shows TPLC derived with the mean mass flow at MFR 1.5 % and x/C_{ax} 1.25 in the passage of non-axisymmetrically contoured endwalls subjected to magnetic fields. The contoured endwall passage revealed elevated aerodynamic performance with lower TPLC values at the MFR of 1.5 % upon the introduction of magnetic flux. The TPLC derived with the mean mass flow of passage showed an identical tendency with magnetic flux. As *Ha* rises, TPLC lowers first, becomes stand still for a while, and rises for an elevated *Ha* of 100. At MFR 1.5 % for contoured endwall, passage possesses inferior aerodynamic losses from *Ha* 25 (1.24 %) to 75 (2.23 %) compared to elevated *Ha*, with hot gas ingression. Hence, *Ha* 75 is the optimal magnetic field strength noticed in this study. The lower TPLC derived with the mean mass flow is because of the weakening of vortices at the leading edge upstream by coolant injection. When MFRs as well as momentum fluxes of coolant injection are elevated, new vortices develop in the upstream location and aerodynamic losses are elevated.

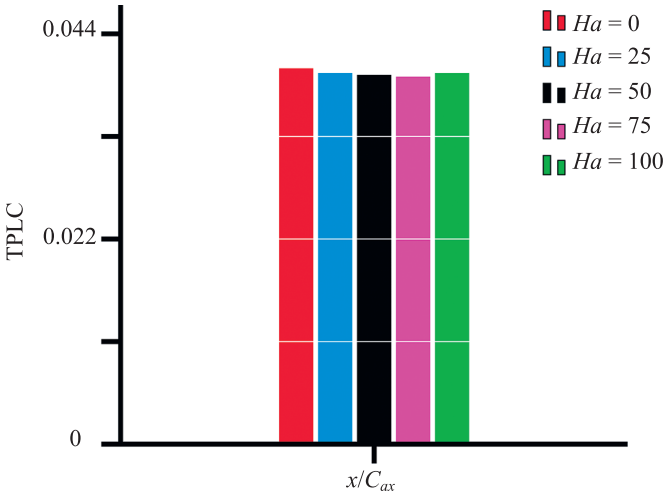

Fig. 6. Impact of magnetic flux on TPLC at x/C_{ax} = 1.25, MFR = 1.5 %

Secondary kinetic energy coefficient at exit

The loss coefficient is an assessment of the depletion of aggregate energy at the turbine downstream flow exit, while C_{ske} represents unavailable kinetic energy at the flow exit. Therefore, C_{ske} is a component measure of the kinetic energy of flow and assesses the anticipated losses due to secondary flow at a specific position and never a replacement for loss. The experimental results concerning flat endwalls had elevated C_{ske} values at the tip position. The association between the calculated and simulated C_{ske} values is outstanding with the exclusion of the findings of the Baldwin-Lomax model [28], with no purpose to acquire perfect vorticity of the flow. The magnitude of divergence between the various shapes of endwalls is five-fold higher in the case of C_{ske}, in comparison to the diversification with respect to the loss coefficient and hence adjudged as the highly validated physical parameter in a flow field to estimate the prospective loss arising from the secondary flow [29].

The non-axisymmetric endwall shape developed for the turbine has strongly lowered exit secondary kinetic energy up to 36 % and 47.4 % for 15 % and 20 % span than the flat endwall. C_{ske} slowly reduces as the span increases from 2.5 % to 20 %. Thereafter it lowers rapidly with an optimal span of 30 % and the lowest after a 40 % span. C_{ske} is elevated alone consequent to the inception of endwall contouring at lower thermal load and originates from the enhanced vigor of the system of the HV. CFD, therefore, can be utilized to forecast the effects of contouring of endwall, amenable with C_{ske} as the significant parameter demonstrated in the current investigation.

Table. Impact of magnetic flux on NHFR at MFR = 1.5 %

x/C_{ax}	*Ha* = 0	*Ha* = 25	*Ha* = 50	*Ha* = 75	*Ha* = 100
0	1.90	1.9300	1.9400	1.950	1.9200
0.65	0.04	0.0406	0.0408	0.041	0.0405
1	0	0	0	0	0

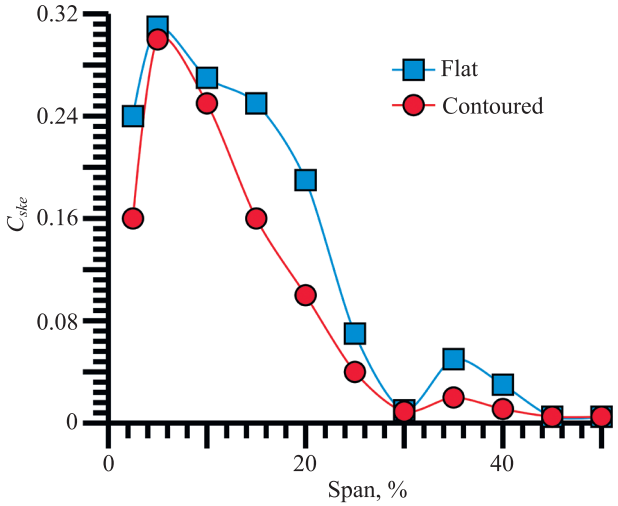

Fig. 7. Comparison between contoured and flat vane endwall at the exit for secondary kinetic energy coefficient

Conclusion

With the magnetohydrodynamic effect, a more uniform distribution of heat transfer performance is achieved, reduced hot spots and thermal damage, and improved the critical component overall efficiency and lifespan. Non-axisymmetric endwall contouring leads to improved net heat flux reduction and aerodynamic performance. It has the potential to reduce the separation bubble size on the endwall of the turbine blade and can lead to the lowering of turbulence and secondary flow, which in turn could augment the turbine efficiency. The level of maximum enhancement benefit of pitch averaged film cooling effectiveness (2.3 %) is noticed around the vane leading edge at *Ha* 75. Increasing the *Ha* from 0 to 75 resulted in an approximately 2.3-fold decrease in the *Nu* on the endwall of a turbine blade as well as enhanced net heat flux reduction (2.63 %) and aerodynamic performance (2.23 %). The optimum magnetic field strength identified for ideal turbine efficiency is *Ha* 75. The coefficient of secondary kinetic energy is demonstrated to be a significant criterion for the contouring of the turbine blade endwall. The paramount advantage of 47.4 % is accomplished for the endwall at a span of 20 % in respect of a non-axisymmetric contoured case in comparison to a flat case.

One of the main challenges is the requirement for a strong magnetic field, which can be difficult and expensive to generate. Additionally, the magnetic field can interfere with the operation of other components in the turbine, which can further complicate the design and implementation of the magnetohydrodynamic system. The passage aft location, entrance boundary layer segregation downstream, the flow field around the upstream cavity in the HV development, and the location of the vortices with respect to the secondary flow away from the endwall need to be explored in designing endwall contours. Revamping the heat transfer forecast of the endwall seems to be the upcoming prime obstacle in enhancing durability and axial turbine efficiency by way of ideal thermal and aerodynamic designs. It may be possible to develop more effective and efficient magnetohydrodynamic systems for turbine endwall contouring.

References

1. Arjun K.S., Tide P.S., Biju N. Optimum profiles of endwall contouring for enhanced net heat flux reduction and aerodynamic performance. *Journal of Harbin Institute of Technology (New Series)*, 2023, in press. https://doi.org/10.11916/j.issn.1005-9113.2023037
2. Krishna M.V., Ahamad N.A., Chamkha A.J. Numerical investigation on unsteady MHD convective rotating flow past an infinite vertical moving porous surface. *Ain Shams Engineering Journal*, 2021, vol. 12, no. 2, pp. 2099–2109. https://doi.org/10.1016/j.asej.2020.10.013
3. Xenos M., Dimas S., Kafoussias N. MHD compressible turbulent boundary-layer flow with adverse pressure gradient. *Acta Mechanica*, 2005, vol. 177, pp. 171–190. https://doi.org/10.1007/s00707-005-0221-7
4. Jaafar A., Waini I., Jamaludin A., Nazar R., Pop I. MHD flow and heat transfer of a hybrid nanofluid past a nonlinear surface stretching/shrinking with effects of thermal radiation and suction. *Chinese Journal of Physics*, 2022, vol. 79, pp. 13–27. https://doi.org/10.1016/j.cjph.2022.06.026
5. Ali A., Kanwal T., Awais M., Shah Z., Kumam P., Thounthong P. Impact of thermal radiation and non-uniform heat flux on MHD hybrid nanofluid along a stretching cylinder. *Scientific Reports*, 2021, vol. 11, pp. 20262. https://doi.org/10.1038/s41598-021-99800-0
6. Mobadersani F., Rezavand A. MHD effect on nanofluid flow and heat transfer in backward-facing step using two-phase model. *AUT Journal of Mechanical Engineering*, 2020, vol. 4, no. 1, pp. 51–66. https://doi.org/10.22060/AJME.2019.14843.5747
7. Loganayagi V., Kameswaran P.K. Magnetohydrodynamic and heat transfer impacts on ferrofluid over a rotating disk: An application to hard disk drives. *Journal of Thermal Science and Engineering Applications*, 2021, vol. 13, no. 1, pp. 011001. https://doi.org/10.1115/1.4047007
8. Nourbakhsh A., Mombeni H., Bayareh M. Effects of radiation and magnetohydrodynamics on heat transfer of nanofluid flow over a

Литература

1. Arjun K.S., Tide P.S., Biju N. Optimum profiles of endwall contouring for enhanced net heat flux reduction and aerodynamic performance // Journal of Harbin Institute of Technology (New Series). 2023. in press. https://doi.org/10.11916/j.issn.1005-9113.2023037
2. Krishna M.V., Ahamad N.A., Chamkha A.J. Numerical investigation on unsteady MHD convective rotating flow past an infinite vertical moving porous surface // Ain Shams Engineering Journal. 2021. V. 12. N 2. P. 2099–2109. https://doi.org/10.1016/j.asej.2020.10.013
3. Xenos M., Dimas S., Kafoussias N. MHD compressible turbulent boundary-layer flow with adverse pressure gradient // Acta Mechanica. 2005. V. 177. P. 171–190. https://doi.org/10.1007/s00707-005-0221-7
4. Jaafar A., Waini I., Jamaludin A., Nazar R., Pop I. MHD flow and heat transfer of a hybrid nanofluid past a nonlinear surface stretching/shrinking with effects of thermal radiation and suction // Chinese Journal of Physics. 2022. V. 79. P. 13–27. https://doi.org/10.1016/j.cjph.2022.06.026
5. Ali A., Kanwal T., Awais M., Shah Z., Kumam P., Thounthong P. Impact of thermal radiation and non-uniform heat flux on MHD hybrid nanofluid along a stretching cylinder // Scientific Reports. 2021. V. 11. P. 20262. https://doi.org/10.1038/s41598-021-99800-0
6. Mobadersani F., Rezavand A. MHD effect on nanofluid flow and heat transfer in backward-facing step using two-phase model // AUT Journal of Mechanical Engineering. 2020. V. 4. N 1. P. 51–66. https://doi.org/10.22060/AJME.2019.14843.5747
7. Loganayagi V., Kameswaran P.K. Magnetohydrodynamic and heat transfer impacts on ferrofluid over a rotating disk: An application to hard disk drives // Journal of Thermal Science and Engineering Applications. 2021. V. 13. N 1. P. 011001. https://doi.org/10.1115/1.4047007
8. Nourbakhsh A., Mombeni H., Bayareh M. Effects of radiation and magnetohydrodynamics on heat transfer of nanofluid flow over a

plate. *SN Applied Sciences*, 2019, vol. 1, pp. 1581. https://doi.org/10.1007/s42452-019-1634-6
9. Ellahi R., Alamri S.Z., Basit A., Majeed A. Effects of MHD and slip on heat transfer boundary layer flow over a moving plate based on specific entropy generation. *Journal of Taibah University for Science*, 2018, vol. 12, no. 4, pp. 476–482. https://doi.org/10.1080/16583655.2018.1483795
10. Ullah H., Hayat T., Ahmad S., Alhodaly M.S., Momani S. Numerical simulation of MHD hybrid nanofluid flow by a stretchable surface. *Chinese Journal of Physics*, 2021, vol. 71, pp. 597–609. https://doi.org/10.1016/j.cjph.2021.03.017
11. Jusoh R., Nazar R., Pop I. Magnetohydrodynamic boundary layer flow and heat transfer of nanofluids past a bidirectional exponential permeable stretching/shrinking sheet with viscous dissipation effect. *ASME Journal of Heat and Mass Transfer*, 2019, vol. 141, no. 1, pp. 012406. https://doi.org/10.1115/1.4041800
12. Yıldız F., Alpman E., Kavurmacioglu L., Camci C. An Artificial Neural Network (ANN) based aerothermal optimization of film cooling hole locations on the squealer tip of an HP turbine blade: preprint. *SSRN Electronic Journal*, 2022. https://doi.org/10.2139/ssrn.4117325
13. Alam T., Kim M-H. A comprehensive review on single phase heat transfer enhancement techniques in heat exchanger applications. *Renewable and Sustainable Energy Reviews*, 2018, vol. 81, pp. 813–839. https://doi.org/10.1016/j.rser.2017.08.060
14. Malvandi A. Film boiling of magnetic nanofluids (MNFs) over a vertical plate in presence of a uniform variable-directional magnetic field. *Journal of Magnetism and Magnetic Materials*, 2016, vol. 406, pp. 95–102. https://doi.org/10.1016/j.jmmm.2016.01.008
15. *Inverse Heat Conduction and Heat Exchangers*. ed. by S. Bhattacharyya, R. Mehta, M.M. Ardekani, R. Biswas. London, UK, IntechOpen Ltd., 2020. http://dx.doi.org./10.5772/intechopen.80096
16. Mahfoud B. Simulation of magnetic field effect on heat transfer enhancement of swirling nanofluid. *International Journal of Computational Materials Science and Engineering*, 2022, vol. 11, no. 4, pp. 2250007. https://doi.org/10.1142/S2047684122500075
17. Arjun K.S., Tide P.S., Biju N. Turbine passage secondary flow dynamics and endwall heat transfer under different inflow turbulence. *Journal of Harbin Institute of Technology (New Series)*, 2023, in press. https://doi.org/10.11916/j.issn.1005-9113.2023042
18. Tsujita H., Mizuki S., Yamamoto A. Numerical investigation of effects of incidence angle on aerodynamic performance of ultra-highly loaded turbine cascade. *Proc. of the ASME Turbo Expo 2006: Power for Land, Sea, and Air, Turbomachinery, Parts A and B. Vol. 6*, 2006, pp. 839–849. https://doi.org/10.1115/GT2006-90939
19. Snedden G.C. *The Application of Non-Axisymmetric Endwall Contouring in a 1½ Stage*, Rotating Turbine: PhD thesis, Durham University, United Kingdom, 2011.
20. Vázquez R., Fidalgo V.J. The effect of Reynolds and Mach number on end-wall profiling performance. *Proc. of the ASME Turbo Expo 2010: Power for Land, Sea, and Air, Turbomachinery, Parts A, B, and C. Vol. 7*, 2010, pp. 1357–1368. https://doi.org/10.1115/GT2010-22765
21. Du K., Jia Y., Song H., Chen L., Zhang Q., Cui T., Liu C. Effect of slot jet flow on non-axisymmetric endwall cooling performance of high-load turbines. *Machines*, 2023, vol. 11, no. 2, pp. 134. https://doi.org/10.3390/machines11020134
22. Schäflein L., Janssen J., Brandies H., Jeschke P., Behre S. Influence of purge flow injection on the performance of an axial turbine with three-dimensional airfoils and non-axisymmetric endwall contouring. *Journal of Turbomachinery*, 2023, vol. 145, no. 6, pp. 061004. https://doi.org/10.1115/1.4056238
23. Menter F.R. Two-equation eddy-viscosity turbulence models for engineering applications. *AIAA — Journal*, 1994, vol. 32, no. 8, pp. 1598–1605. https://doi.org/10.2514/3.12149
24. Menter F.R., Langtry R.B., Likki S.R., Suzen Y.B., Huang P.G., Völker S. A correlation-based transition model using local variables — Part I: Model formulation. *Journal of Turbomachinery*, 2006, vol. 128, no. 3, pp. 413–422. https://doi.org/10.1115/1.2184352
25. Lynch S.P., Thole K.A. Heat transfer and film cooling on a contoured blade endwall with platform gap leakage. *Journal of Turbomachinery*, 2017, vol. 139, no. 5, pp. 051002. https://doi.org/10.1115/1.4035202
26. Ingram G. *Endwall Profiling for the Reduction of Secondary Flow in Turbines*. PhD thesis. Durham University, United Kingdom, 2003.
27. Bai B., Li Z., Li J., Mao S., Ng W.F. The effects of axisymmetric convergent contouring and blowing ratio on endwall film cooling and

plate // SN Applied Sciences. 2019. V. 1. P. 1581. https://doi.org/10.1007/s42452-019-1634-6
9. Ellahi R., Alamri S.Z., Basit A., Majeed A. Effects of MHD and slip on heat transfer boundary layer flow over a moving plate based on specific entropy generation // Journal of Taibah University for Science. 2018. V. 12. N 4. P. 476–482. https://doi.org/10.1080/16583655.2018.1483795
10. Ullah H., Hayat T., Ahmad S., Alhodaly M.S., Momani S. Numerical simulation of MHD hybrid nanofluid flow by a stretchable surface // Chinese Journal of Physics. 2021. V. 71. P. 597–609. https://doi.org/10.1016/j.cjph.2021.03.017
11. Jusoh R., Nazar R., Pop I. Magnetohydrodynamic boundary layer flow and heat transfer of nanofluids past a bidirectional exponential permeable stretching/shrinking sheet with viscous dissipation effect // ASME Journal of Heat and Mass Transfer. 2019. V. 141. N 1. P. 012406. https://doi.org/10.1115/1.4041800
12. Yıldız F., Alpman E., Kavurmacioglu L., Camci C. An Artificial Neural Network (ANN) based aerothermal optimization of film cooling hole locations on the squealer tip of an HP turbine blade: preprint // SSRN Electronic Journal. 2022. https://doi.org/10.2139/ssrn.4117325
13. Alam T., Kim M-H. A comprehensive review on single phase heat transfer enhancement techniques in heat exchanger applications // Renewable and Sustainable Energy Reviews. 2018. V. 81. P. 813–839. https://doi.org/10.1016/j.rser.2017.08.060
14. Malvandi A. Film boiling of magnetic nanofluids (MNFs) over a vertical plate in presence of a uniform variable-directional magnetic field // Journal of Magnetism and Magnetic Materials. 2016. V. 406. P. 95–102. https://doi.org/10.1016/j.jmmm.2016.01.008
15. Inverse Heat Conduction and Heat Exchangers / ed. by S. Bhattacharyya, R. Mehta, M.M. Ardekani, R. Biswas. London, UK, IntechOpen Ltd., 2020. http://dx.doi.org/10.5772/intechopen.80096
16. Mahfoud B. Simulation of magnetic field effect on heat transfer enhancement of swirling nanofluid // International Journal of Computational Materials Science and Engineering. 2022. V. 11. N 4. P. 2250007. https://doi.org/10.1142/S2047684122500075
17. Arjun K.S., Tide P.S., Biju N. Turbine passage secondary flow dynamics and endwall heat transfer under different inflow turbulence // Journal of Harbin Institute of Technology (New Series). 2023. in press. https://doi.org/10.11916/j.issn.1005-9113.2023042
18. Tsujita H., Mizuki S., Yamamoto A. Numerical investigation of effects of incidence angle on aerodynamic performance of ultra-highly loaded turbine cascade // Proc. of the ASME Turbo Expo 2006: Power for Land, Sea, and Air, Turbomachinery, Parts A and B. Vol. 6. 2006. P. 839–849. https://doi.org/10.1115/GT2006-90939
19. Snedden G.C. The Application of Non-Axisymmetric Endwall Contouring in a 1½ Stage, Rotating Turbine: PhD thesis. Durham University, United Kingdom, 2011.
20. Vázquez R., Fidalgo V.J. The effect of Reynolds and Mach number on end-wall profiling performance // Proc. of the ASME Turbo Expo 2010: Power for Land, Sea, and Air, Turbomachinery, Parts A, B, and C. Vol. 7. 2010. P. 1357–1368. https://doi.org/10.1115/GT2010-22765
21. Du K., Jia Y., Song H., Chen L., Zhang Q., Cui T., Liu C. Effect of slot jet flow on non-axisymmetric endwall cooling performance of high-load turbines // Machines. 2023. V. 11. N 2. P. 134. https://doi.org/10.3390/machines11020134
22. Schäflein L., Janssen J., Brandies H., Jeschke P., Behre S. Influence of purge flow injection on the performance of an axial turbine with three-dimensional airfoils and non-axisymmetric endwall contouring // Journal of Turbomachinery. 2023. V. 145. N 6. P. 061004. https://doi.org/10.1115/1.4056238
23. Menter F.R. Two-equation eddy-viscosity turbulence models for engineering applications // AIAA — Journal. 1994. V. 32. N 8. P. 1598–1605. https://doi.org/10.2514/3.12149
24. Menter F.R., Langtry R.B., Likki S.R., Suzen Y.B., Huang P.G., Völker S. A correlation-based transition model using local variables - Part I: Model formulation // Journal of Turbomachinery. 2006. V. 128. N 3. P. 413–422. https://doi.org/10.1115/1.2184352
25. Lynch S.P., Thole K.A. Heat transfer and film cooling on a contoured blade endwall with platform gap leakage // Journal of Turbomachinery. 2017. V. 139. N 5. P. 051002. https://doi.org/10.1115/1.4035202
26. Ingram G. Endwall Profiling for the Reduction of Secondary Flow in Turbines: PhD thesis. Durham University, United Kingdom, 2003.
27. Bai B., Li Z., Li J., Mao S., Ng W.F. The effects of axisymmetric convergent contouring and blowing ratio on endwall film cooling and

vane pressure side surface phantom cooling performance. *Journal of Engineering for Gas Turbines and Power*, 2022, vol. 144, no. 2, pp. 021020. https://doi.org/10.1115/1.4052500
28. Versteeg H.K., Malalasekera W. *An Introduction to Computational Fluid Dynamics*. The Finite Volume Method. Pearson Prentice Hall, 1995, 503 p.
29. Snedden G., Dunn D., Backstrom V.T.W., Ingram G. Observations on the selection of objective function for the optimisation of turbine endwalls using computational fluid dynamics. *Proc. of the 7th South African Conference on Computational and Applied Mechanics (SACAM)*, 2010, pp. 574–588.

vane pressure side surface phantom cooling performance // Journal of Engineering for Gas Turbines and Power. 2022. V. 144. N 2. P. 021020. https://doi.org/10.1115/1.4052500
28. Versteeg H.K., Malalasekera W. An Introduction to Computational Fluid Dynamics. The Finite Volume Method. Pearson Prentice Hall, 1995. 503 p.
29. Snedden G., Dunn D., Backstrom V.T.W., Ingram G. Observations on the selection of objective function for the optimisation of turbine endwalls using computational fluid dynamics // Proc. of the 7th South African Conference on Computational and Applied Mechanics (SACAM). 2010. P. 574-588.

Authors

Kozhikkatil Sunil Arjun — PhD, Post Doctoral Fellow, Cochin University of Science and Technology, Kochi, 682022, India, sc 57205762026, https://orcid.org/0000-0003-1832-3759, arjunks@cusat.ac.in

Porathoor Sunny Tide — PhD, Professor, Cochin University of Science and Technology, Kochi, 682022, India, sc 57216868077, https://orcid.org/0000-0002-8061-113X, tideps@cusat.ac.in

Авторы

Арджун Кожиккатил Сунил — PhD, докторант, Кочинский университет науки и технологий, Кочи, 682022, Индия, sc 57205762026, https://orcid.org/0000-0003-1832-3759, arjunks@cusat.ac.in

Тайд Поратур Санни — PhD, профессор, Кочинский университет науки и технологий, Кочи, 682022, Индия, sc 57216868077, https://orcid.org/0000-0002-8061-113X, tideps@cusat.ac.in

Received 27.09.2023
Approved after reviewing 01.11.2023
Accepted 17.11.2023

Статья поступила в редакцию 27.09.2023
Одобрена после рецензирования 01.11.2023
Принята к печати 17.11.2023